

DEVELOPMENT OF A MODEL AND COMPUTER CODE TO DESCRIBE SOLAR GRADE SILICON PRODUCTION PROCESSES



FIFTH QUARTERLY REPORT

R. SRIVASTAVA AND R.K. GOULD

FEBRUARY 1979

The JPL Low-Cost Solar Array Project is sponsored by the U. S. Department of Energy and forms part of the Solar Photovoltaic Conversion Program to initiate a major effort toward the development of low-cost solar arrays. This work was performed for the Jet Propulsion Laboratory, California Institute of Technology by agreement between NASA and DoE.

(NASA-CR-158601) DEVELOPMENT OF A MODEL AND COMPUTER CODE TO DESCRIBE SOLAR GRADE SILICON PRODUCTION PROCESSES Quarterly Report (AeroChem Research Labs., Inc.) 36 p HC A03/MF A01 N79-23514 Unclas 25172 CSCI 10A G3/44

AeroChem Research Laboratories, Inc.
Princeton, New Jersey

This report was prepared as an account of work sponsored by the United States Government. Neither the United States nor the United States Department of Energy, nor any of their employees, nor any of their contractors, subcontractors, or their employees, makes any warranty, express or implied, or assumes any legal liability or responsibility for the accuracy, completeness or usefulness of any information, apparatus, product or process disclosed, or represents that its use would not infringe privately owned rights.

**DEVELOPMENT OF A MODEL
AND COMPUTER CODE TO
DESCRIBE SOLAR GRADE SILICON
PRODUCTION PROCESSES**

FIFTH QUARTERLY REPORT
R. SRIVASTAVA AND R. K. GOULD
FEBRUARY 1979

JPL Contract No. 954862
DRL Item No. 4, DRD No. QR
LSA Silicon Material Task

Approved by 
Hartwell F. Calcote
Director of Research

AeroChem **Research Laboratories, Inc.**
Princeton, New Jersey

FOREWORD AND ACKNOWLEDGMENTS

This report covers the period 1 October 1978 to 31 December 1978. During this period, D.B. Olson and P.J. Howard contributed to the program.

One of the authors (RS) wishes to express his gratitude to Professor D.E. Rosner of Yale University, for many helpful discussions pertaining to transport properties, and to R. Israel (Yale University) for providing Chapman-Enskog theory estimates of α_{∞} .

ABSTRACT

This program aims at developing mathematical models, and computer codes based on these models, which will allow prediction of the product distribution in chemical reactors in which gaseous silicon compounds are converted to condensed-phase silicon. The reactors to be modeled are flow reactors in which silane or one of the halogenated silanes is thermally decomposed or reacted with an alkali metal, H_2 or H atoms. Because the product of interest is particulate silicon, processes which must be modeled, in addition to mixing and reaction of gas-phase reactants, include the nucleation and growth of condensed Si via coagulation, condensation, and heterogeneous reaction.

During this report period computer codes were developed and used to calculate (i) coefficients for Si vapor and Si particles describing transport due to concentration and temperature gradients (i.e., Fick and Soret diffusion, respectively), and (ii) estimates of thermochemical properties of Si n-mers. The former are needed to allow the mass flux of Si to reactor walls to be calculated. Because of the extremely large temperature gradients that exist in some of the reactors to be used in producing Si (particularly the Westinghouse reactor), it was found that thermal (Soret) diffusion can be the dominant transport mechanism for certain sizes of Si particles. The thermochemical estimates are required to allow computation of the formation rate of Si droplets. With the completion of these calculations the information and coding of the particle routines in the modified LAPP code is at the point where debugging can be done and that is now in progress.

~~XXXXXXXXXX~~ PAGE BLANK NOT FILLED

TABLE OF CONTENTS

	<u>Page</u>
ABSTRACT	iii
I. INTRODUCTION	1
II. SILICON TRANSPORT LAWS AND IMPLICATIONS	1
III. DESCRIPTION OF THE TRANSPORT COEFFICIENTS	4
A. Universal Formula for D_i	6
B. Universal Formula for α_i	9
C. Transport Properties	11
1. General Trends	11
2. Pressure and Temperature Dependences	12
3. Need for Effective Transport Properties	13
4. Relative Importance of Various Transport Mechanisms	14
5. Particle Size Range over which Soret Transfer Dominates	15
6. Conclusions	16
IV. DESCRIPTION OF THERMODYNAMIC PROPERTIES	17
A. Silicon n-mer Thermochemistry	17
B. Other Work	18
V. PLANS	18
VI. NEW TECHNOLOGY	19
VII. REFERENCES	19

LIST OF TABLES

<u>Table</u>		
I	COMPARISON OF VARIOUS SIZE RELATED VARIABLES FOR Si-Ar	21
II	VALUES OF SOME INPUT AND COMPUTED CONSTANTS	22
III	THERMODYNAMIC PROPERTIES OF Si N-MERS USING A CLASSICAL LIQUID DROP MODEL	24
IV	THERMODYNAMIC PROPERTIES OF Si N-MERS USING THE MODEL OF REFERENCE 22	25

LIST OF FIGURES

<u>Figure</u>		<u>Page</u>
1	VARIATION OF DEPOSITION RATE OF SILICON PARTICLES WITH SIZE	26
2	RATIONALE FOR THE DIFFUSIVITY FORMULA (EQ. (5))	26
3	VARIATION OF α_i AND D_i FOR "LARGE" PARTICLES	27
4	VARIATION OF α_i AND D_i FOR "SMALL" PARTICLES	28
5	VARIATION OF α_i AND D_i WITH PRESSURE AND TEMPERATURE	29
6	COMPARISON OF THE SORET FACTOR α_i FOR TWO DIFFERENT TYPES OF CARRIER GASES	30

I. INTRODUCTION

This program aims at developing mathematical models, and computer codes based on these models, which will allow prediction of the product distribution, as a function of time, in chemical reactors in which gaseous silicon compounds are converted to condensed-phase silicon. The reactors to be modeled are flow reactors in which silane or one of the halogenated silanes is thermally decomposed or reacted with alkali metals. Because the product of major interest is condensed-phase silicon, the models considered must allow calculation of particle formation (via chemical reaction followed by nucleation), and the growth rate of the particulate Si via coagulation, condensation, and heterogeneous reaction. Since the efficiency of the particulate Si collection process will depend on the particle size distribution of the Si, this must also be computed.

During this quarter the following problems have received attention: (i) continued development of computational schemes for calculating heat and mass fluxes to walls of reactors in which SiX_n/M ($X = \text{halide}$, $M = \text{alkali metal}$) flames are occurring, (ii) development of nucleation models by which $\text{Si}(\ell)$ particles are formed from $\text{Si}(\text{g})$, (iii) continued development of detailed chemical kinetic mechanisms describing the formation of free Si ($\text{Si}(\text{g})$) by these flames, and (iv) development of coagulation and condensation models by which the $\text{Si}(\ell)$ particle growth is calculated. The bulk of this report concerns the development of models used to obtain the various transport coefficients needed to allow Si mass fluxes (as $\text{Si}(\text{g})$ and as $\text{Si}(\ell)$ droplets) to reactor walls. Particular attention is paid to the role of thermal (Soret) diffusion which, because of the extremely large temperature gradients and the size of Si droplets that may be encountered in these reactors, needs investigation. Finally, the methods used to estimate the thermochemical properties of Si n-mers, needed to implement the Si nucleation model, are outlined. Short discussions of work on (iii) and (iv) above are also included.

II. SILICON TRANSPORT LAWS AND IMPLICATIONS

The mechanism of deposition of silicon particles onto reactor walls is dependent on the size of the particles. For particles larger than about a micron, deposition is controlled by turbulence-induced inertial impaction; sub-micron sized silicon droplets deposit by a convective-diffusion process.

In order to predict the mass flux to the reactor wall of the latter class of droplets it is necessary to recognize two separate contributions to the time-averaged diffusional flux: (i) a concentration gradient-driven (Fick) flux and (ii) a temperature gradient-driven (Soret) flux. The relative importance of these contributions itself varies with particle size, the former being dominant for the smaller sub-micron sizes while the latter controls the behavior of particles with sizes closer to a micron, as shown qualitatively in Fig. 1. Thus, in general,¹⁻³ for a species i (vapor or particle) that is dilute in a carrier gas the diffusional mass flux (per unit area, per unit time) at any point, \vec{j}_i'' , (corresponding to a particular pressure and temperature) is given by^{1,2}:

$$\vec{j}_i'' = -\rho D_i \left[(\nabla \vec{Y}_i) + \alpha_i Y_i (1 - Y_i) \frac{1}{T} (\nabla T) \right] + \vec{j}_{\text{turb}}'' \quad (1)$$

where ρ is the local mass density of the carrier gas, Y_i the local mass fraction of the diffusion species, T the local absolute temperature (with the operator ∇ denoting gradient of the particular scalar, temperature or concentration). The first two terms in Eq. (1) represent the diffusional mass fluxes due to concentration and temperature gradients, respectively. The third term, \vec{j}_{turb}'' , is the mass flux contribution due to turbulent or "eddy diffusion."⁴ Assuming, as is customary, that the turbulent diffusion also has a Fickian nature, one can write.

$$\vec{j}_{\text{turb}}'' = -\rho \epsilon_p (\nabla \vec{Y}_i) \quad (2)$$

where ϵ_p is the so-called "eddy diffusivity." Particles larger than about a micron would inevitably be deposited on the walls due to inertial impaction caused by turbulent velocity fluctuations normal to the wall. Hence, for such large particles the overall mass flux to the wall would be dominated by \vec{j}_{turb}'' . However, the sub-micron size particles will be driven close to the wall by turbulence eddies before the concentration and temperature gradient driven fluxes (i.e., Fick and Soret effects) become important in the final stages of deposition, within a nearly laminar (viscous) sublayer next to the wall.

However, before deposition rate (or mass flux) can be calculated, one needs to establish the Fick (or Brownian) diffusion coefficient D_i , the dimensionless thermal (Soret) diffusion or "thermophoretic" factor α_i , and the "eddy" diffusivity ϵ_p . The former two transport property coefficients depend upon the molecular nature of the species present in a given "effective" binary mixture

(e.g., silicon-argon, in the case considered later in this report), and on the prevailing pressure and temperature.* In addition, they are both strong functions of particle size, changing by several orders of magnitude (as shown later) in traversing the particle size spectrum from molecular diameters[†] to about a micron.

Interestingly enough, while the values of the Fick diffusivities (i.e., D_i and ϵ_p) are always positive, ensuring that Brownian and turbulent transport of Si always occurs in the direction of decreasing concentration (towards the reactor walls), the value of α_i may sometimes be negative. The latter circumstance is usually characteristic of diffusing species that are lighter than the carrier gas (e.g., silicon vapor (28.09) diffusing through argon (39.94)). Thus the Soret flux has the potential to drive silicon vapor towards higher temperatures, away from the "cool" walls, and thereby reduce the overall collection efficiency of Si.¹ Fortunately, as shown later, the value of α_i for Si particles (defined here as any molecular cluster exceeding roughly twice the mass of a single vapor molecule) is invariably positive, since the particles are heavier than the surrounding gas. That is, while condensed Si droplets will always be driven towards the reactor walls, uncondensed Si vapor could actually be driven away from the walls due to the Soret effect. In this report, therefore, in addition to considering the mechanisms of Brownian and turbulent transport of silicon, we investigate the conditions under which Soret, or temperature gradient-driven diffusion, can be important. Although this latter effect has been ignored in the past in the belief that its contribution to the overall mass flux would be negligible, we conclude that the Soret effect can indeed play a crucial role in the Si (particle/vapor) separation process, under typical reactor conditions. Fortunately, the Soret (or thermophoretic) flux for condensed Si droplets will always favor deposition onto the walls. The detrimental tendency of this flux to oppose deposition of any uncondensed Si vapor can be minimized, as shown later, by enriching the reactor with a light gas like H₂, which tends to drive the system towards a condition of positive "effective thermal diffusion."

* Under typical silicon reactor operating conditions the concentration dependence of these transport coefficients will be negligible, due to the diluteness of silicon in the carrier gas.

[†] Particle size is described in terms of diameter or radius since it will be assumed here that the particles (silicon liquid droplets) are perfectly spherical.

III. DESCRIPTION OF THE TRANSPORT COEFFICIENTS

For the sake of comparison, it is necessary to define the "eddy" diffusivity, ϵ_p , for mass transport. In general, by viewing turbulence as the random agitated movement of small packets of fluid, it is possible to define ϵ_p in terms of a "mixing length" (in much the same spirit as the "viscous mean-free-path" in the kinetic theory of gases represents an average distance for effective transfer of momentum by molecules). Thus,

$$\epsilon_p \sim u' \lambda_1 \sim \lambda_1^2 \left| \frac{dU}{dy} \right|$$

where λ_1 is a mixing length, u' the large scale turbulent velocity fluctuations present in the core flow of the reactor, and $\left| \frac{dU}{dy} \right|$ the magnitude of the time-averaged (steady) normal velocity gradient. Both λ_1 and $\left| \frac{dU}{dy} \right|$ will vary with distance above a wall, y , with λ_1 being zero at the wall since turbulence is precluded (i.e., the "no-slip" condition). While the many available models of turbulence provide different expressions for the variation of λ_1 with distance normal to a wall, accurate estimates of λ_1 and the proportionality constant in the above expression, for any given flow situation, usually result from experiments. Lin et al³ suggest the following expression, valid in the viscous sublayer flow, next to a wall:

$$\epsilon_p = \nu \left(\frac{y^+}{14.5} \right)^3, \quad y^+ < 5 \quad (3)$$

where ν is the kinematic viscosity and y^+ is a non-dimensional normal distance from the wall defined as:

$$y^+ \equiv \left[y U (f/2)^{1/2} \right] / \nu \quad (4)$$

with U the average velocity and f the Fanning friction factor. For particles small enough to follow the small-scale eddy motions close to a wall, the eddy diffusivity does not depend upon particle size.

Although silicon particles of widely varying sizes must be considered in the modeling of the deposition processes within any proposed reactor, reliable information about the "molecular" transport coefficients (i.e., D_i and α_i) is available only at the two extremes of the size spectrum. For particle sizes

much smaller than the mean-free-path of the carrier gas, the well-known kinetic theory results of Chapman and Enskog⁶ (CE) apply. In this limit of "free-molecule" flow, surrounding gas molecules do not suffer appreciable changes in their distribution functions upon collision with the particle. Furthermore, since expressions for α_1 are an outcome of CE theory using second-order terms of the perturbation series, while the D_1 expressions come out of first-order terms, one concludes that α_1 will be more sensitive to interactions between colliding molecules. Thus more sophisticated molecular potential models than the Lennard-Jones 12:6 (e.g., the exponential model)^{7,8} might ultimately be necessary to accurately determine α_1 in this limit, although the Lennard-Jones might suffice for engineering purposes.

For particles much larger than the mean-free-path of the surrounding gas, the gas structure becomes "invisible" and the behavior can be described by the Navier-Stokes equations for a "continuum," subject to the usual "no-slip" boundary conditions at the particle surface (e.g., the Stokes-Einstein (SE) expression for particle diffusivity⁹).

The main difficulty in specifying transport properties is encountered for particles in the intermediate size range, on the order of a mean-free-path. This presents the notorious unsolved problem of the "transition regime." Although several attempts have been made to extend the continuum results into the transition regime, by imposing "slip" or jump-type boundary conditions at the particle surface, these are at best heuristic. Understanding of the real transition mechanisms involved is altogether insufficient. However, the transition regime experimental data of Millikan¹⁰ and others have made it possible to establish various empirical correction factors (as discussed later) that cover a wide portion of the transition regime. Unfortunately, even such widely used interpolation formulae as the Stokes-Einstein-Millikan (SEM) expression are unsatisfactory since they do not exactly match the predictions of CE theory when extended to the "free-molecule" limit.

Crucial to the accurate modeling of silicon deposition, therefore, is a proper description of the abovementioned transport coefficients. Since present knowledge regarding the "transition regime" is insufficient, it would be justifiable to suggest universal interpolation formulae for these coefficients.

covering the entire particle size (or Knudsen number*) range. Moreover, mathematically continuous functions that blend together the known results in different regions would be both physically and computationally more desirable.

In what follows, a novel rational approach² to creating such "universal" descriptions of the Fick diffusivity (i.e., D_i) and the Sorlet factor (i.e., α_i) is outlined. Finally, some numerical results are presented to demonstrate the validity of the proposed formulae under conditions typical of a silicon reactor.⁴

A. UNIVERSAL FORMULA FOR D_i

The expression for diffusivity adopted in this report blends the near-continuum SEM relation (valid for small Kn_i values) with the free-molecule CE expression (valid for large values of Kn_i , > 10) according to the following universally valid relationship:

$$D_i = D_{SEM} + \frac{D_{CE} - D_{SEM}}{[1 + \exp\{-C(Kn_i - Kn_0)\}]} \quad (5)$$

where C and Kn_0 are constants. The magnitude of C controls the abruptness of the transition from D_{SEM} to D_{CE} as the Kn_i is increased. Kn_0 is the Knudsen number value at the "point of inflection" of D_{SEM} .⁹ Figure 2 illustrates the rationale behind choosing such an interpolation function to describe the diffusivity of particles in a gas.

The Stokes-Einstein-Millikan expression for diffusivity, D_{SEM} , is based on Maxwell's¹⁰ famous oil-drop experiments which permitted measurement of the internal drag force on particles of various sizes moving through a gas. Using a stochastic analysis of Brownian motion, Einstein¹¹ had earlier related the particle diffusivity to the "mobility," or relative velocity per unit force,

* The particle Knudsen number (Kn_i) will be defined here as the ratio of the mean-free-path (λ) in the surrounding gas to the particle radius (R_i) (i.e., $Kn_i \equiv \frac{\lambda}{R_i}$). Thus $Kn_i \rightarrow 0$ corresponds to the "continuum" limit while $Kn_i \rightarrow \infty$ refers to the "free-molecule" limit. It is sometimes assumed⁹ that the range $0 < Kn_i < 0.25$ represents the region of "slip-flow" while $0.25 < Kn_i < 10$ is the region of "transition-flow."

through the well-known relation:

$$D_i = kTB \quad (6)*$$

the mobility, B, being given by the Stokes formula for low Reynolds number continuum flow around a sphere:

$$B = \frac{1}{6\pi\eta R_i} \quad (7)$$

where η is the dynamic viscosity of the gas. Recognizing that as the particle size approaches the gas mean-free-path, the drag for a given velocity becomes less (due to "slip") than predicted by Stokes law (i.e., the mobility increases), Millikan suggested the following expression for mobility, which is a well-accepted correction of the Stokes result:

$$B = \frac{1}{6\pi\eta R_i \varepsilon} \quad (7a)$$

where

$$\varepsilon \equiv [1 + C_m Kn_i + C_d Kn_i \exp(-0.88/Kn_i)]^{-1} \quad (7b)$$

$$C_m \equiv (2 - \alpha_m)/\alpha_m \quad (7c)$$

$$C_d \equiv \left\{ \frac{7}{8} \alpha_m^2 + \left(\frac{13}{4} \right) \alpha_m - 2 \right\} / \left\{ \alpha_m + \frac{7}{8} \alpha_m^2 \right\} \quad (7d)$$

with α_m denoting the so-called momentum accommodation coefficient, a measure of the efficiency of momentum transfer between the particle and the surrounding gas molecules.⁺ Combining Eqs. (6) through (7d) yields the needed expression for diffusivity, valid at least for small departures from $Kn_i = 0$:

* k is the Boltzmann constant.

⁺ Values of α_m depend on the nature of the particle and the surrounding gas. Experimentally determined values for various substances⁹ usually lie in the range $0.9 < \alpha_m < 1.0$. In this report $\alpha_m = 1$ (perfect accommodation) is assumed for the results presented later.

$$D_{SEM} = \frac{kT}{6\pi\mu R_i} [1 + C_m Kn_i + C_d Kn_i \exp(-0.88/Kn_i)] \quad (8)$$

At the other extreme, for particles much smaller than the gas mean-free-path (but not necessarily as small as molecules) the diffusivity D_{CE} should be given by the Chapman-Enskog relation¹²:

$$D_{CE} = 1.8583 \times 10^{-3} \left(\frac{T^{3/2}}{p} \right) \left(\frac{1}{M_c} + \frac{1}{M_i} \right)^{1/2} \left(\frac{1}{\sigma_{ci}^2 \Omega} \right) \quad (9)$$

where p is the pressure (atm), M_c and M_i the molecular weights of the carrier gas, c , and diffusing molecular species, i , respectively, σ_{ci} the effective collision diameter (angstroms) and Ω the reduced collision integral. Equation (9) is strictly valid only for molecules with spherically symmetric potential force fields, with the supplementary relations:

$$\sigma_{ci} = \frac{1}{2} (\sigma_c + \sigma_i)$$

$$\Omega = \text{fn} \left(\frac{kT}{\epsilon_{ci}} \right) \quad (\text{See Ref. 13 for a tabulation of this function.}) \quad (10)$$

$$\epsilon_{ci} = (\epsilon_c \epsilon_i)^{1/2}$$

where σ_{ci} and ϵ_{ci} can be taken to represent the size and energy-well depth in, say, the Lennard-Jones molecular interaction model.

To generalize Eq. (9) for the case of small particles, we need to redefine only the molecular weight M_i and the molecular diameter σ_i . Treating the particle as a "heavy molecule," g times the mass of the corresponding molecule, its "molecular weight" can be expressed as:

$$M_i = g M_1 = \left[\left(\frac{4}{3} \pi R_i^3 \right) \left(\frac{N_A \rho_i}{M_1} \right) \right] M_1 \quad (11)*$$

* N_A is the Avogadro number.

where M_1 is the molecular weight of the substance constituting the particle, g is the ratio of the particle volume to the molecular volume (i.e., $\frac{M_1}{N_A \rho_1}$) of the substance, and ρ_1 is the particle density. The "molecular" diameter of a particle is simply

$$\sigma_1 = (2R_1) \times 10^8 \text{ (Å)} \quad (12)$$

if the particle radius R_1 is expressed in centimeters. Combining Eqs. (9) through (12) yields the following expression for the diffusivity of very small particles:

$$D_{CE} = 1.8583 \times 10^{-3} \left(\frac{T^{3/2}}{P} \right) \left(\frac{1}{M_c} + \frac{1}{gM_1} \right)^{1/2} \left(\frac{1}{\sigma_{c1}^2 \Omega} \right) \quad (13)$$

where

$$\sigma_{c1}^2 \cong \frac{1}{4} (\tau_c + 2 \times 10^8 R_1)^2 \quad (13a)$$

$$\Omega = 1.22 \left(\frac{kT}{\epsilon_1} \right)^{-0.16} \quad (13b)$$

$$g = \left(\frac{4}{3} \pi R_1^3 \right) \left(\frac{N_A \rho_1}{M_1} \right) \quad (13c)$$

Incorporating the expressions for D_{SEM} and D_{CE} , given by Eqs. (8) and (13), into Eq. (5) yields the required, universally valid, equation for the diffusivity D_1 . The value of Kn_0 was taken to be 0.44 so that the point of inflection in Eq. (5) coincided with the inflection point of the SEM formula (i.e., Eq. (8)). The value of C was chosen to be 1.5 for the results presented below.

B. UNIVERSAL FORMULA FOR α_1

Using a rationale similar to the one adopted for D_1 , but necessarily different because entirely different (and more complicated) expressions usually describe α_1 , we propose the following universally valid formula for the Soret factor:

$$\alpha_i = \left(\frac{A Kn_i}{1 + A Kn_i} \right) \alpha_\infty + \left(\frac{1}{1 + A Kn_i} \right) \alpha_0 \quad (14)$$

where α_∞ is the "thermal diffusion factor" predicted by CE theory for $Kn_i \rightarrow \infty$ and α_0 is the value of the Soret factor as $Kn_i \rightarrow 0$. The constant A is determined by forcing the prediction of Eq. (14), in the transition regime, to agree with established experimental data for some value of Kn_i of order unity.

It is known that a particle suspended in a gas with a uniform temperature gradient will drift through the gas under the action of a thermal force. When this "thermophoretic" force just balances the opposing drag force on the particle, a constant thermal settling velocity is achieved. Using Millikan's oil-drop apparatus, modified to provide for a temperature gradient, Phillips¹⁴ was able to accurately describe the thermal settling velocity up to $Kn_i \approx 0(1)$, for particles of widely varying thermal conductivities (including the coupling that usually exists between the velocity and temperature fields surrounding a moving particle). We have incorporated² the Phillips formulae into a computer program that predicts the thermal settling velocity (\vec{V}_T) at some value of the Knudsen number (say, $Kn_i = 1$) and used this to find the corresponding Soret factor (α_p). Knowing α_∞ and α_0 , as shown below, A can then be determined as:

$$A = \frac{1 - \alpha_0}{\alpha_\infty - \alpha_p} \quad (15)$$

for a given particle-carrier gas combination and given flow conditions.

Since the CE expression for α_∞ is extremely complicated, we utilize the analysis of Waldmann and Schmitt¹⁵ which yields the following expression for \vec{V}_T valid for small particles whose drift in a temperature gradient can be associated with the stronger bombardment by higher energy molecules from the "hot side":

$$\frac{\vec{V}_T}{\left[-\frac{1}{T} (\vec{\nabla}T) \right]} \equiv \alpha_i D_i = \frac{3}{4} \nu \left(\frac{1}{1 + \frac{\pi}{8} \alpha_d} \right) = \alpha_\infty D_i$$

where D_i is the diffusivity already discussed, ν the kinematic viscosity, and α_d the fraction of molecules that undergo "diffused reflection" from the particle surface. It turns out that the above result for α_i does not exactly

match the CE result for molecular sized particles. In order to achieve this match a new constant correction factor σ_{corr} is introduced as follows:

$$\alpha_{\infty} = \frac{3}{4} \left(\frac{v}{D_i} \right) \frac{1}{\left(1 + \frac{\pi}{8} \alpha_d \right)} \frac{1}{\sigma_{\text{corr}}} \quad (16)$$

Physically, the effect of σ_{corr} is to account for the variation in α_d with increasing particle size.* The ratio (v/D_i) is the particle Schmidt number (Sc_i). It is a measure of the relative importance of momentum to mass transfer. Since the diffusivity of large particles is small, unlike gas molecules, Sc_i is typically large (as seen later, Table I).

Here α_0 is taken to be related to the thermophoretic velocity deduced by Epstein,¹⁵ for particles much larger than the gas mean-free-path (using a slip-flow procedure). Using Epstein's result one can write:

$$\alpha_0 = \frac{3}{4} Sc_i \left[\frac{1}{1 + 0.5(\lambda_i/\lambda_c)} \right] \quad (17)$$

where λ_i and λ_c are the thermal conductivities of the particle and gas, respectively.

Equations (15), (16), and (17) when incorporated into Eq. (14) provide the required universal formula for the Soret factor α_i .

C. TRANSPORT PROPERTIES

1. General Trends

The analysis just presented for the evaluation of the transport properties of particles dilute in a carrier gas, was first applied to the case of silicon particles in argon, under typical reactor operating conditions. Figures 3 and 4 show the numerically computed values of α_i and D_i over a wide range of Knudsen number (Kn_i). Table I is provided to gain an idea of the corresponding particle size in terms of the other possible size variables: g , R_i , or Sc_i . Note that while g and R_i are absolute measures

* When $(\alpha_i)_{\text{CE}}$ is negative, $\sigma_{\text{corr}} \approx 1$ may be assumed.

of particle size, Kn_i and Sc_i depend strongly upon the prevailing pressure and temperature. Table II gives the values of input constants and the computed values of some useful quantities. The following features regarding Figs. 3 and 4 are also noteworthy:

(i) Both D_i and α_i change rapidly by orders of magnitude, in going from very small ($g = 1$, $R_i = 1.58 \text{ \AA}$, $Kn_i = 4.4 \times 10^3$, $Sc_i = 0.73$) to large particles ($g=10^{10}$, $R_i = 157 \text{ \mu m}$, $Kn_i = 4.4 \times 10^{-3}$, $Sc_i = 4.6 \times 10^9$). In this connection it should be mentioned that particles of about 1 \mu m diam (see Fig. 1 and Table I), which lie within the "transition regime," correspond to the size ranges:

$$\begin{aligned} 10^{10} &< g < 10^{11} \\ \times 10^{-3} \text{ cm} &< R_i < 7.3 \times 10^{-3} \text{ cm} \\ 2.04 &> Kn_i > 0.95 \\ 1.1 \times 10^6 &< Sc_i < 5.35 \times 10^6 \end{aligned}$$

(ii) As expected physically, the diffusivity D_i of large particles is small, increasing significantly as particles approach molecular dimensions. On the other hand, the magnitude of the Soret factor α_i shows an opposite trend in this case. The physical implication¹ of this is better understood from Eq. (1), which gives the net mass flux. Since D_i is always positive a negative α_i (or temperature gradient) tends to reduce the flux. In this case, the usually large α_i when D_i is small, and vice versa, leads to the conclusion that the Soret flux will dominate the Brownian flux only for larger particles.

2. Pressure and Temperature Dependences

Figure 5 reveals the pressure and temperature dependences of the transport coefficients. Due to the complicated functional dependence of α_i and D_i on Kn_i and Sc_i , simple representations may not be possible for all particle sizes. It is clear, however, that over the range of temperatures (≈ 1700 to 3500 K) and pressures (≈ 0.5 to 1.0 atm) of interest in silicon reactors, D_i retains approximately the same characteristics as described by the $T^{3/2}/\rho$ expression (i.e., $T^{3/2}/\rho$), at least for particle diameters up to about 1 \mu m . On the other hand, α_i is nearly insensitive to temperature and pressure. Figure 5 is restricted to particle diameters up to about a micron since it is generally true that the Soret effect (thermophoresis) may not

be as significant as inertial forces for very large particles.

3. Need for Effective Transport Properties

Figure 6 compares the case of a negative α_i (e.g., Si vapor in Ar) versus one with a positive α_i (e.g., Si vapor in H₂).^{*} In order to increase the separation (or collection) efficiency of silicon, it is clear that α_i should be positive so that the Soret flux is directed towards the "cold" reactor walls. Since a multicomponent mixture of gases is actually present an "effective" Soret factor must be considered such that

$$\alpha_{i,\text{eff}} = \left[\sum_{j \neq i} \alpha_{ij} x_j \right] / (1 - x_i) \quad (18)$$

where x_i is the mole fraction of species i and α_{ij} the Soret factor for species i diffusing in a carrier gas j . It is to be noted that the "effective" Soret factor depends both on the relative concentrations of the various gaseous species present as well as on the magnitude and sign of their individual Soret factors. Typically, as in the Westinghouse process,¹⁶ for instance, one can expect a mixture of silicon in mainly sodium chloride vapor, argon, and hydrogen gases. The various mole fractions would be roughly

$$\begin{aligned} x_{\text{Si}} &= 0.08 \\ x_{\text{H}_2} &= 0.5 \\ x_{\text{Ar}} &= 0.12 \\ x_{\text{NaCl}} &= 0.3 \end{aligned}$$

If the effective carrier gas is a mixture of H₂, Ar, and NaCl its average molecular weight would be

$$M_{\text{avg}} = \sum_j x_j M_j = 23.34 \quad (19)$$

Since the molecular weight of Si vapor molecules is larger than this ($M_{\text{Si}} \approx 28$) one would expect a positive value of $\alpha_{i,\text{eff}}$ to govern the Soret diffusion of

* Note, the value of α_i for Si particles in both Ar and H₂ is positive.

silicon vapor in a mixture of the abovementioned gases. Indeed, using the above mole-fraction estimates together with the following approximate values of α (deduced from CE theory) applicable to Si vapor:

$$\begin{aligned}\alpha_{\text{Si,H}_2} &= 0.7 \\ \alpha_{\text{Si,NaCl}} &= -0.3 \\ \alpha_{\text{Si,Ar}} &= -0.1\end{aligned}$$

one obtains $\alpha_{i,\text{eff}} \cong 0.27$. Thus the net Soret flux of vapor should normally be directed towards the wall. Using this it was estimated that the Soret mass flux for Si vapor to the reactor wall may not exceed 15-20% of the corresponding Fick flux. However, the sign of $\alpha_{i,\text{eff}}$ is sensitive to the prevailing product concentrations. It is conceivable, therefore, that in certain portions, near the reactor walls, the concentration of H_2 may be locally small enough for $\alpha_{i,\text{eff}}$ to become negative and lead to a detrimental flux of Si vapor away from the walls.* To eliminate the occurrence of such a possibility we would recommend maintaining a H_2 rich atmosphere near the reactor walls at all times.

Finally, it is worth pointing out that the real problem, as mentioned earlier, involves (besides vapor) some silicon droplets that may be treated as "heavy molecules" (i.e., the submicron size class). In the context of the above discussion, pertaining to vapor, it is clear that the effective "molecular weight" of this "heavy-molecule-gas" will always be considerably greater than that of Si vapor (see Eq. (11)). Hence, one can, in fact, expect a huge (but favorable) Soret contribution to the overall mass flux for particles in the "transition regime."

4. Relative Importance of Various Transport Mechanisms

Finally, one needs to gain some idea of the relative importance of the three mechanisms of diffusion (i.e., Brownian, Soret, and turbulent) studied in this report. Brownian and turbulent diffusion are known to be important for very small and very large particles, respectively. However,

* Our more exact boundary layer calculations in the future will also be aimed at determining the extent of this possibility.

the importance of Soret diffusion for particles of about a micron diameter is easily seen from Fig. 5. Typically, α_i is large ($\approx 10^3$) while D_i is small ($\approx 10^{-9}$). Recalling that α_i , the Soret factor, is related to a thermal diffusion coefficient $D_{T,i}$ (which is really the appropriate counterpart of D_i), the following useful "thermal diffusion ratios" may be defined:

$$k_T \equiv \frac{D_{T,i}}{\rho D_i} \approx \alpha_i Y_i (1 - Y_i) \quad (20)$$

$$k'_T \equiv \frac{D_{T,i}}{\rho(D_i + \epsilon_p)} \approx \frac{D_{T,i}}{\rho \epsilon_p} \approx \frac{\alpha_i D_i Y_i (1 - Y_i)}{\epsilon_p} \quad (21)$$

The former compares the extent of Soret and Brownian diffusion, whereas the latter expresses the importance of Soret vs overall Fickian (i.e., Brownian + turbulent) diffusion. Since, as seen above, $\alpha_i D_i \approx 1$, $Y_i \approx 0.1$, and $\epsilon_p \approx 10^{-2}$ (from Eq. (3)), close to the wall,* one finds:

$$k_T \approx 10^4$$

$$k'_T \approx 10$$

That is, Soret transport of silicon particles will predominate all the other forms of diffusion for particles about 1 μ m diam, in a viscous sublayer region close to the reactor wall.

5. Particle Size Range Over Which Soret Transfer Dominates

It is of interest to determine here the particle size "window" (see Fig. 1) for which Soret diffusion dominates. An upper limit is approximately set by the physical requirement that particles exceeding about 1 μ m diam will be controlled solely by their inertia.⁹ However, the condition $k_T = 1$ (see Eq. (20)) determines the lower size limit at which Soret diffusion becomes as important as Brownian diffusion. It is interesting to note that this lower limit is sensitive to the prevailing Si concentration (or mass fraction).

* Note that since $\epsilon_p \approx y^3$, the value of ϵ_p drops rapidly as the wall is approached. For $0 < y^+ < 5$, the variation in ϵ_p corresponds to $0 < \epsilon_p < 0.15$ (see Table II).

Using $Y_1 \approx 0.1$, one obtains $\alpha_1 \approx 10$, which (from Fig. 5) corresponds to a particle diameter of $0.01 \mu\text{m}$, under typical reactor conditions. With $k_T = 10$ one can expect Soret diffusion to outweigh Brownian diffusion, a condition which here would correspond to $\alpha_1 = 100$ and a particle diam of $0.02 \mu\text{m}$. Thus one can safely say that Soret diffusion (i.e., thermophoresis) will be the dominant transport mechanism, near the reactor walls, for silicon droplets in the size range: $0.01 \mu\text{m}$ to $1.0 \mu\text{m}$ diam. Note that this is a much wider size range than the one usually quoted in the literature on a somewhat ad hoc basis.

6. Conclusions

The analysis just presented emphasizes the following aspects relevant to modeling the silicon separation processes within a reactor:

(a) It is essential that the model describe the transport to the reactor walls of a whole size distribution of silicon particles, from vapor molecules to droplets of several microns in diameter. As a first step to determining the average mass flux due to a statistical particle size distribution, the universally valid transport coefficient formulae, developed in this report, will be needed.

(b) Very small or large silicon droplets will be deposited on the reactor walls by Brownian and turbulent diffusion, respectively. However, the often ignored transport mechanism of Soret diffusion (or thermophoresis), due to large temperature gradients, will control the deposition of silicon droplets in the diameter range $0.01 \mu\text{m}$ to $1.0 \mu\text{m}$, within a viscous sublayer region close to the walls.

(c) Unlike the Brownian and turbulent diffusivities, the Soret factor can possibly take on negative values, rendering the Soret flux of silicon vapor to be directed away from the reactor walls. For silicon droplets, however, since this factor is inevitably positive, Soret diffusion invariably favors deposition onto the walls. It is to be noted that while the Soret flux of silicon vapor in a typical reactor may not exceed 15-20% of the prevailing Fick flux, close to the reactor walls, the contribution of the Soret effect to the overall mass flux of silicon droplets far outweighs all other diffusion mechanisms (as pointed out in (b) above). To eliminate the possible occurrence of a detrimental Soret flux of uncondensed silicon vapor in local regions close to the reactor walls, we recommend that a hydrogen-rich atmosphere be maintained within the reactor at all times.

IV. DESCRIPTION OF THERMODYNAMIC PROPERTIES

A. SILICON N-MER THERMOCHEMISTRY

In this report period we have also concentrated efforts on obtaining a set of thermodynamic data which will allow us to model the formation of Si(l) from Si(g) in a reasonable fashion. The chemical kinetic model we are using¹⁷ requires values of the heat capacity, c_p , the enthalpy ($H_T - H_{298}$), the free energy function $-(G^\circ - H_{298}^\circ)/T$, and the heat of formation, ΔH_f° , for each Si n-mer. Such data do not exist and must therefore be estimated. Two approaches have been chosen. The first uses a very naive chemical model to estimate the unknown quantities; it assumes that the heat capacity of each n-mer is simply the heat capacity of Si(l) times the number of Si atoms in the n-mer. The free energy function is obtained by assuming that the free energy of the n-mer is the sum of the molar free energy of the liquid (times n) and the molar surface energy, G_s , where, from the Kelvin eq.,¹⁸

$$G_{s,n} = \frac{2}{3} (4 \pi r_n \sigma_{Si} N_A) \quad (22)$$

In this equation r_n is the radius of the n-mer and is assumed to be that of a liquid drop of Si containing n Si atoms with a density ρ_{Si} , given by¹⁹

$$\rho_{Si} = 3.02 - 0.35 \times 10^{-3} (T - 273.15), \text{ gm ml}^{-1} \quad (23)$$

The surface tension of Si liquid, σ_{Si} , is given by²⁰

$$\sigma_{Si} = 720[1.67 - 0.67 (T/1685)^{1.2}] \text{ ergs cm}^{-2} \quad (24)$$

No attempt is made to enforce self-consistency in the model, i.e., the entropy is not the integral of the heat capacity divided by T. The thermodynamic data in Table III are examples estimated using this model. Generally the model seems to suffer from underestimating the entropy (and thus overestimating free energy functions), making it less than zero (and thus not physically reasonable) at lower temperatures. However, this model does have the virtue of converging towards the thermodynamic properties of the liquid, as it should. Thus for large n-mers and high temperatures the model will be realistic.

The second model used to estimate n-mer thermodynamic data is that of Bauer and Frurip²² also described in Refs. 17 and 23. This model can be expected to yield more realistic values of thermodynamic properties of n-mers where $n \leq 100$ and at low temperatures since the use of the bulk liquid surface energy is avoided. However, it does not guarantee convergence to the liquid thermodynamic properties at large n and, as can be seen in Table IV, the value of the free energy function actually moves away from the bulk liquid values as n increases. The strength of the model is obviously at low values of n where the classical model gives physically unrealistic results. Thus, for now, for $n < 100$ we will use the Bauer model estimates. For $n > 100$ we switch to the classical model. These thermodynamic data, together with estimates of reaction rates obtained using the Bauer and Frurip kinetics model²² are currently being used to compute Si n-mer growth in SiCl_4/Na flames.

Since it is evident that universal formulae of the type discussed earlier, in connection with the transport coefficients, will ultimately be needed to describe the thermodynamic properties as well, such efforts are currently being pursued.²⁴

B. OTHER WORK

The last quarterly report²⁵ described the development of detailed mechanisms to conserve computer run time. Further work during this quarter on simplifying the original 25 step reaction schemes²⁵ for these flames has reduced the number of reaction steps necessary to describe these flames to 13. Reactions involving mixing of SiX_m species and H-atom stripping reactions ($\text{H} + \text{SiX}_m \rightarrow \text{SiX}_{m-1} + \text{HX}$) do not appear to play an important role in the overall reaction scheme which yields free Si.

The particle growth model is now inserted in the LAPP code¹⁷ and debugging of this model has begun.

V. PLANS

During the next quarter, the SiCl_4/Na reaction scheme, the Si n-mer thermochemical estimates, and the Si particle transport coefficients obtained in this quarter will be used to calculate heat and Si mass fluxes to walls in reactors like those being designed by Westinghouse¹⁶ and AeroChem.²⁰ To do this we will be using the LAPP code,¹⁷ now modified

to treat particle nucleation and coagulation in an enclosed reactor. The code is in the debugging stage. To obtain more detailed wall heat and mass flux estimates than are possible with the modified LAPP code we will be relying on the boundary layer code^{1,2,4,27} which specifically examines the crucial region close to the wall.

VI. NEW TECHNOLOGY

No reportable items of new technology have been identified.

VII. REFERENCES

1. Srivastava, R. and Rosner, D.E., "A New Approach to the Correlation of Boundary Layer Mass Transfer Rates with Thermal Diffusion and/or Variable Properties," Int. J. Heat Mass Trans. (in press).
2. Srivastava, R. and Rosner, D.E., "Falsification of Particle Size Distribution for Capture by Simultaneous Brownian Motion and Thermophoresis," Int. J. Heat Mass Trans. (to be submitted).
3. Rosner, D.E., "Thermal (Soret) Diffusion Effects on Interfacial Mass Transport Rates," J. Physicochemical Hydrodynamics, 1, No. 1 (in press).
4. Srivastava, R., "Modeling the Characteristics of High Purity Silicon Production Processes" (in preparation).
5. Lin, C.S., Moulton, R.W., and Putnam, G.L., Ind. Eng. Chem. 45, 640 (1953).
6. Chapman, S. and Cowling, T.G., The Mathematical Theory of Non-Uniform Gases (Cambridge University Press, Cambridge, 1952).
7. Svehla, R.A., "Estimated Viscosities and Thermal Conductivities of Gases at High Temperature," NASA Tech Rept. R-132, 1962.
8. Grew, K.W. and Ibbs, T.C., Thermal Diffusion in Gases (Cambridge University Press, Cambridge, 1952).
9. Hidy, G.M. and Brock, J.R., Dynamics of Aerocolloidal Systems (Pergamon Press, New York, 1970).
10. Millikan, R.A., Phys. Rev. 22, 1 (1923).
11. Einstein, A., Ann. Physik 17, 549 (1905); see also Investigations on the Theory of Brownian Movement, R. Furth, Ed., (Dover, New York, 1956).
12. Bird, R.B., Stewart, W.E., and Lightfoot, E.N., Transport Phenomena (John Wiley, New York, 1960).

13. Hirschfelder, J.O., Curtiss, C.F., and Bird, R.B., Molecular Theory of Gases and Liquids (John Wiley, New York, 1954).
14. Phillips, W.F., "Motion of Aerosol Particles in a Temperature Gradient," Phys. Fluids 18, 144 (1975).
15. Waldmann, L. and Schmitt, K.H., "Thermophoresis and Diffusiophoresis of Aerosols," Aerosol Science, C.N. Davies, ed. (Academic Press, New York, 1966) Chap. VI.
16. Fey, M.B., "Development of a Process for High Capacity Arc Heater Production of Silicon for Solar Arrays," Westinghouse Electric Corp., Quarterly Report, DOE/JPL 954589-78/6, April-June 1978.
17. Gould, R.K., "Development of a Model and Computer Code to Describe Solar Grade Silicon Production Processes," First Quarterly Report, AeroChem TN-184, February 1978.
18. Acamson, A.W., Physical Chemistry of Surfaces (Interscience, New York, 1967) Chap. 2.
19. Glasor, M.V., Liquid Semiconductors (Plenum Press, New York, 1969).
20. Keck, P.H. and Van Horn, W., "Surface Tension of Liquid Silicon and Germanium," Phys. Rev. 91, 511 (1953).
21. JANAF Thermochemical Tables, Dow Chemical Co., Midland MI, continuously updated.
22. Bauer, S.H. and Frurip, D.J., "Homogeneous Nucleation in Metal Vapors. A Self-Consistent Kinetic Model," J. Phys. Chem. 81, 1015 (1977).
23. Gould, R.K., "Development of a Model and Computer Code to Describe Solar Grade Silicon Production Processes," Third Quarterly Report, AeroChem TN-195, ERDA/JPL 954862 78/3, August 1978.
24. Srivastava, R. and Gould, R.K., "Rational Thermodynamic and Transport Property Schemes for Silicon Vapor and Particles" (in preparation).
25. Gould, R.K., "Development of a Model and Computer Code to Describe Solar Grade Silicon Production Processes," Fourth Quarterly Report, AeroChem TN-200, DOE/JPL 954862-78/4, November 1978.
26. Olson, D.B. and Miller, W.J., "Silicon Halide-Alkali Metal Flames as a Source of Solar Grade Silicon," Sixth Quarterly Report, AeroChem TN-201, DOE/JPL 954777-79/6, January 1979.
27. Patankar, S.V. and Spalding, D.B., Heat and Mass Transfer in Boundary Layers (Intertext Books, London, 1970).

TABLE I
 COMPARISON OF VARIOUS SIZE RELATED VARIABLES FOR Si-Ar
 (p = 1 atm, T = 2200 K)

<u>E</u>	<u>R_i (cm)</u>	<u>Kn_i</u>	<u>Sc_i</u>
1.00	1.58 (-08)	4.39 (03)	7.2 (-01)
1.00 (01)	3.39 (-08)	2.04 (03)	2.4
1.00 (02)	7.31 (-08)	9.50 (02)	7.8
1.00 (03)	1.57 (-07)	4.41 (02)	2.3 (01)
1.00 (04)	3.39 (-07)	2.04 (02)	1.1 (02)
1.00 (05)	7.31 (-07)	9.50 (01)	5.2 (02)
1.00 (06)	1.57 (-06)	4.41 (01)	2.3 (03)
1.00 (07)	3.39 (-06)	2.04 (01)	1.0 (04)
1.00 (08)	7.31 (-06)	9.50	4.9 (04)
1.00 (09)	1.57 (-05)	4.41	2.3 (05)
1.00 (10)	3.39 (-05)	2.04	1.1 (06)
1.00 (11)	7.31 (-05)	9.50 (-01)	5.3 (06)
1.00 (12)	1.57 (-04)	4.41 (-01)	2.1 (07)
1.00 (13)	3.39 (-04)	2.04 (-01)	6.8 (07)
1.00 (14)	7.31 (-04)	9.50 (-02)	1.7 (08)
1.00 (15)	1.57 (-03)	4.41 (-02)	4.2 (08)
1.00 (16)	3.39 (-03)	2.04 (-02)	9.5 (08)
1.00 (17)	7.31 (-03)	9.50 (-03)	2.1 (09)
1.00 (18)	1.57 (-02)	4.41 (-03)	4.5 (09)

TABLE II
VALUES OF SOME INPUT AND COMPUTED CONSTANTS

INPUT CONSTANTS (Si-Ar)

P	= 1 atm	
T	= 2200 K	
α_m	= 1.0	
α_d	= 1.0	
M_i	= 28.09	} gm/gm-mol
M_c	= 39.94	
α_∞	= -0.10279	(CE theory estimate)
N_A	= 6.023×10^{23}	molecules/gm-mol
k	= 1.3805×10^{-16}	ergs K ⁻¹
σ_i	= 2.910 Å	
(ϵ_i/k)	= 3036.0 K	
σ_c	= 3.542 Å	
(ϵ_c/k)	= 93.3 K	
λ_i/λ_c	= 350	
C	= 1.5	} (See Eq. (5))
Kn_o	= 0.44	

Particle density: $\rho_i = \rho_{mp} [1 - Z(T - T_{mp})]$

$$\rho_{mp} = 3.025 \text{ gm cm}^{-3}$$

$$Z = 1.175 \times 10^{-4}$$

$$T_{mp} = 1685 \text{ K}$$

Gas Viscosity: $\frac{\mu}{\mu_r} = \left(\frac{T}{T_r}\right)^\omega$

$$\mu_r = 8.021 \times 10^{-4} \text{ poise}$$

$$T_r = 2000 \text{ K}$$

$$\omega = 0.35$$

TABLE II (Continued)

COMPUTED CORRECTION FACTORS

C_m	= 1.0	} (see Eq. (8))
C_d	= 0.61557	
A	= 1.9182	(see Eq. (14))

COMPUTED VALUES OF SOME VARIABLES

ν	= 3.7498 cm ² s ⁻¹
ρ	= 2.2116 × 10 ⁻⁶ gm cm ⁻³
l	= 6.9572 × 10 ⁻⁵ cm
λ_c	= 1.5472 × 10 ⁻⁶ cal/(cm-s-K)

TABLE III
 THERMODYNAMIC PROPERTIES OF Si N-MERS
 USING A CLASSICAL LIQUID DROP MODEL^a

<u>n</u>	<u>c_p/n cal mol⁻¹K⁻¹ (Si atom)⁻¹</u>	<u>$-(G^\circ - H_{298}^\circ)/nT$ cal mol⁻¹K⁻¹ (Si atom)⁻¹</u>	<u>$(H_T - H_{298})/n$ kcal mol⁻¹ (Si atom)⁻¹</u>
1000 K			
6	6.5	- 2.74	4.56
12	6.5	0.70	4.56
24	6.5	3.43	4.56
48	6.5	5.60	4.56
96	6.5	7.32	4.56
∞ (liquid) ^b	6.5	13.93	4.56
2000 K			
6	6.5	11.65	11.06
12	6.5	12.85	11.06
24	6.5	13.80	11.06
48	6.5	14.56	11.06
96	6.5	15.16	11.06
∞ (liquid) ^b	6.5	17.47	11.06
3000 K			
6	6.5	17.70	17.56
12	6.5	18.13	17.56
24	6.5	18.47	17.56
48	6.5	18.74	17.56
96	6.5	18.96	17.56
∞ (liquid) ^b	6.5	19.78	17.56

^a $\Delta H_f^\circ_{298}/n$ for all n-mers is 11.585 kcal mol⁻¹ (Si atom)⁻¹.

^b From Ref. 21.

TABLE IV
THERMODYNAMIC PROPERTIES OF Si N-MERS
USING THE MODEL OF REFERENCE 22

<u>n</u>	<u>c_p/n cal mol⁻¹K⁻¹ (Si atom)⁻¹</u>	<u>$-(G^0 - H_{298}^0)/nT$ cal mol⁻¹K⁻¹ (Si atom)⁻¹</u>	<u>$(H_T - H_{298})/n$ kcal mol⁻¹ (Si atom)⁻¹</u>
1000 K			
6	4.83	16.97	3.93
12	4.83	16.90	3.93
24	4.83	17.64	3.93
48	4.83	18.72	3.93
96	4.83	19.88	3.93
∞ (liquid) ^a	6.5	13.93	4.56
2000 K			
6	5.44	19.89	8.87
12	5.44	19.81	8.87
24	5.44	20.56	8.87
48	5.44	21.64	8.87
96	5.44	22.80	8.87
∞ (liquid) ^a	6.5	17.47	11.06
3000 K			
6	5.28	21.75	14.31
12	5.28	21.74	14.31
24	5.28	22.43	14.31
48	5.28	23.51	14.31
96	5.28	24.62	14.31
∞ (liquid) ^a	6.5	19.78	17.56
298.15 K			
<u>n</u>	<u>$\Delta H_f^0/n$ kcal mol⁻¹ (Si atom)⁻¹</u>		
6	73.00		
12	63.23		
24	55.01		
48	48.09		
96	42.29		
∞ (liquid)	11.59		

^a From Ref. 21.

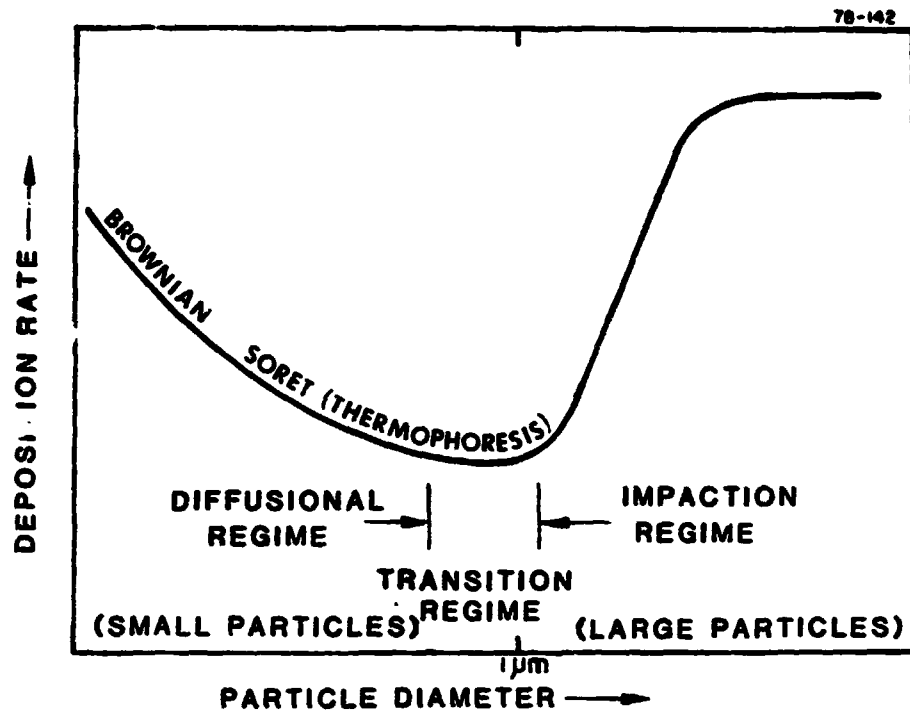


FIGURE 1 VARIATION OF DEPOSITION RATE OF SILICON PARTICLES WITH SIZE

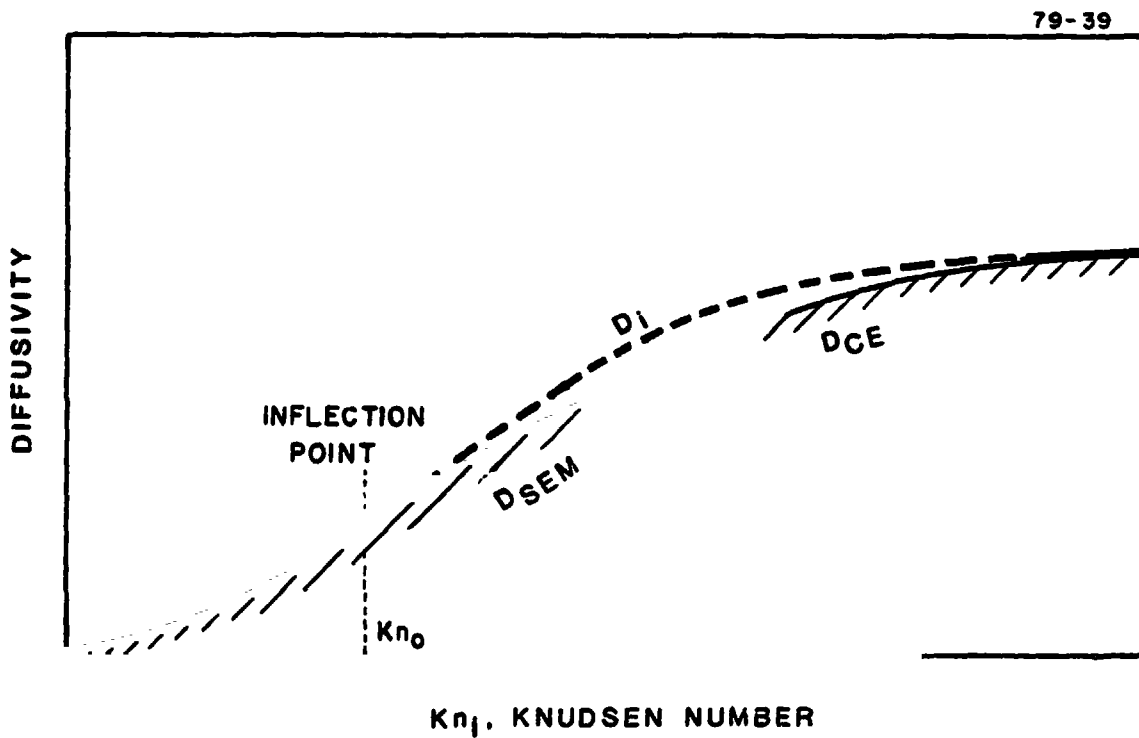


FIGURE 2 RATIONALE FOR THE DIFFUSIVITY FORMULA (EQ. (5))

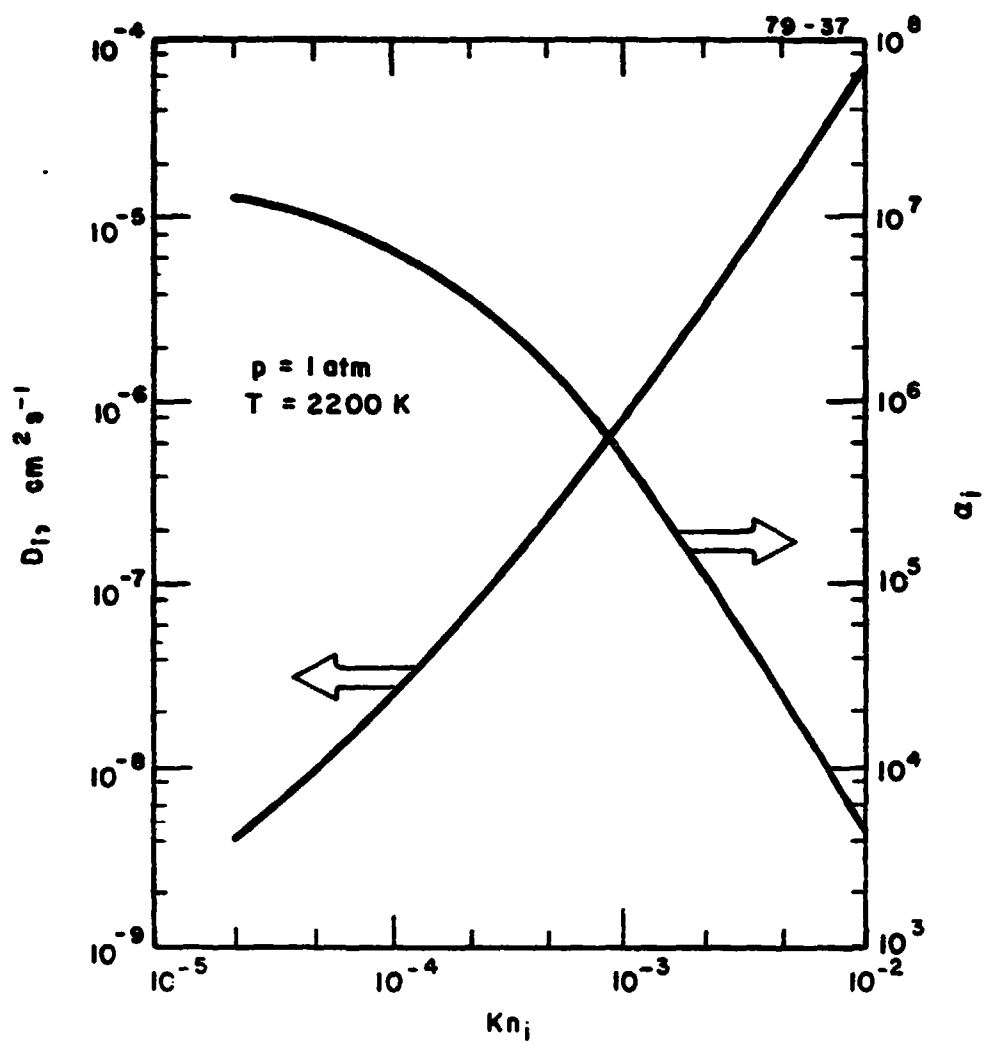


FIGURE 3 VARIATION OF α_i AND D_i FOR "LARGE" PARTICLES

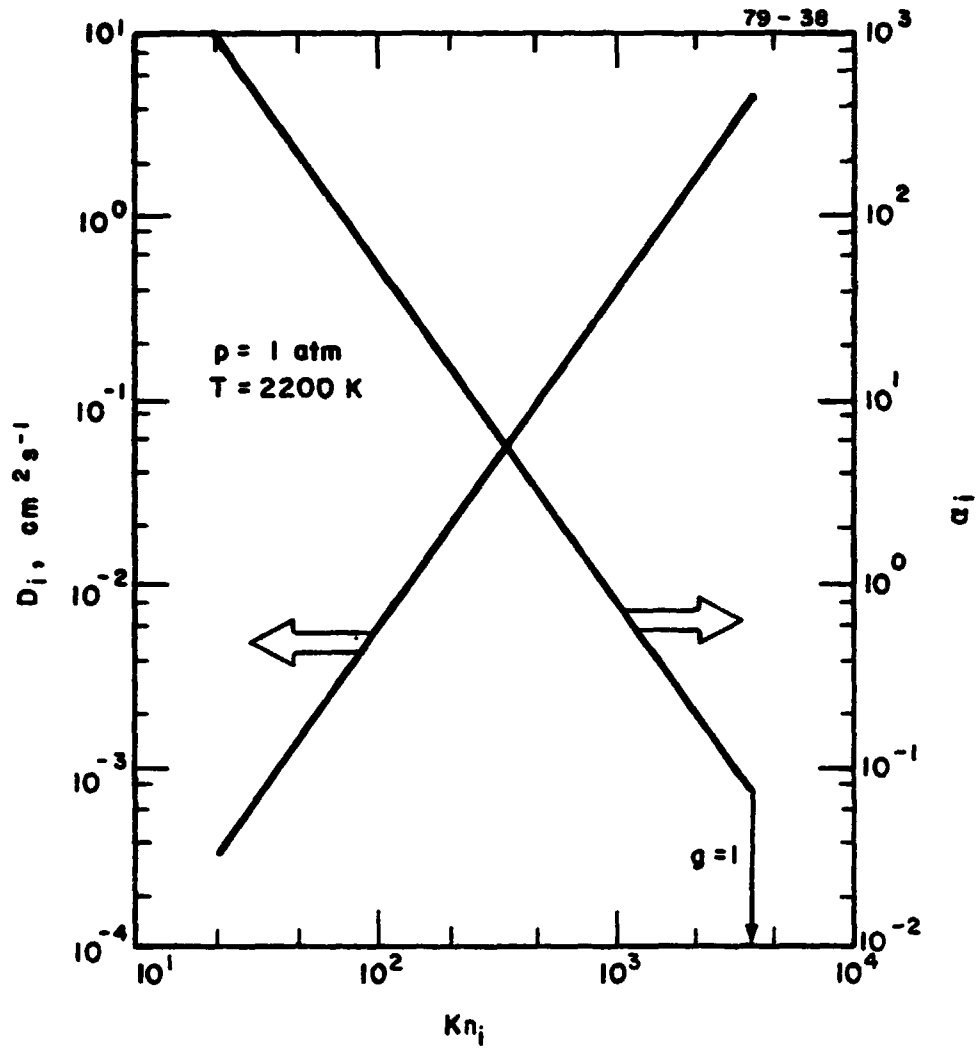


FIGURE 4 VARIATION OF α_i AND D_i FOR "SMALL" PARTICLES
(Note the apparent discontinuity in α_i in going from vapor to particles).

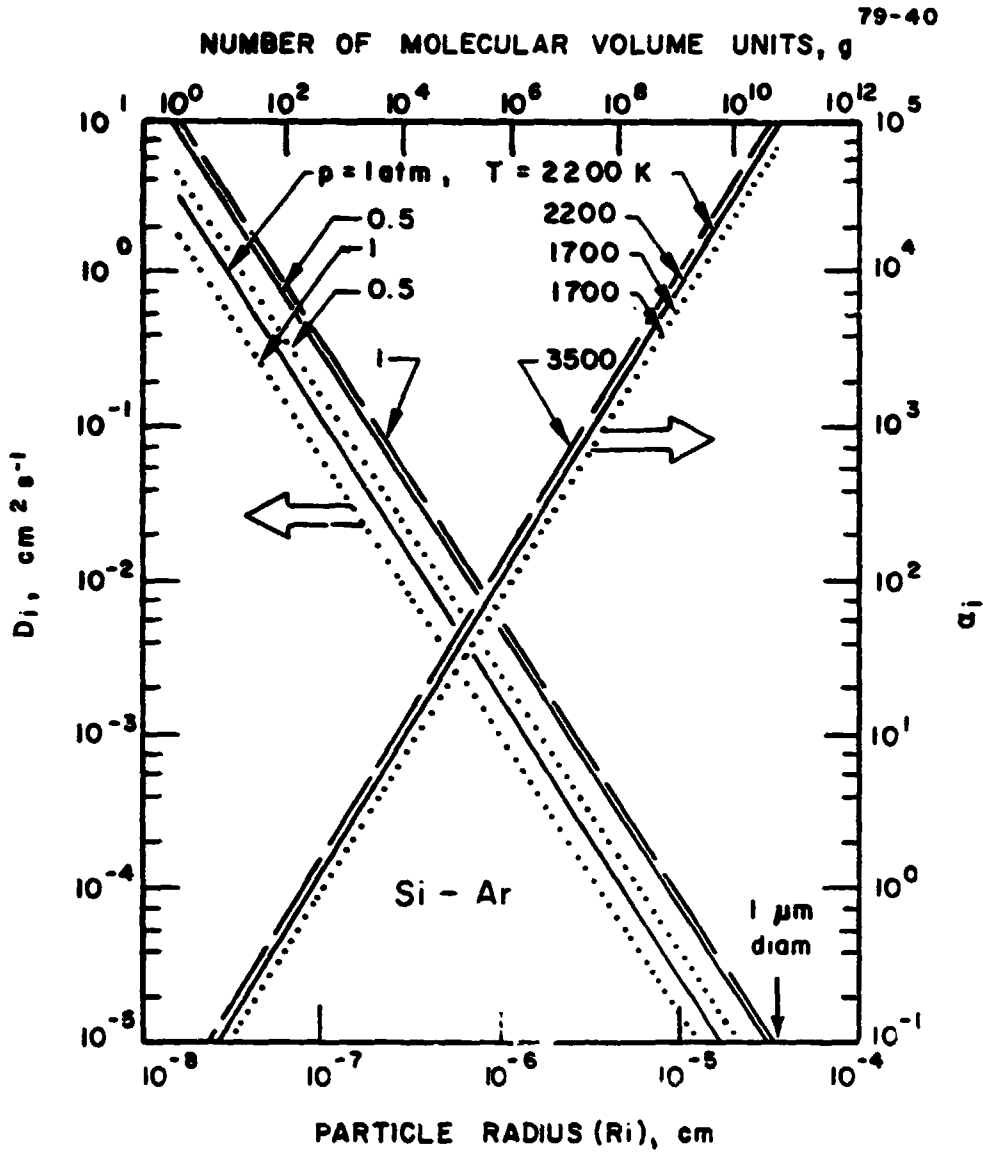


FIGURE 5 VARIATION OF α_1 AND D_1 WITH PRESSURE AND TEMPERATURE

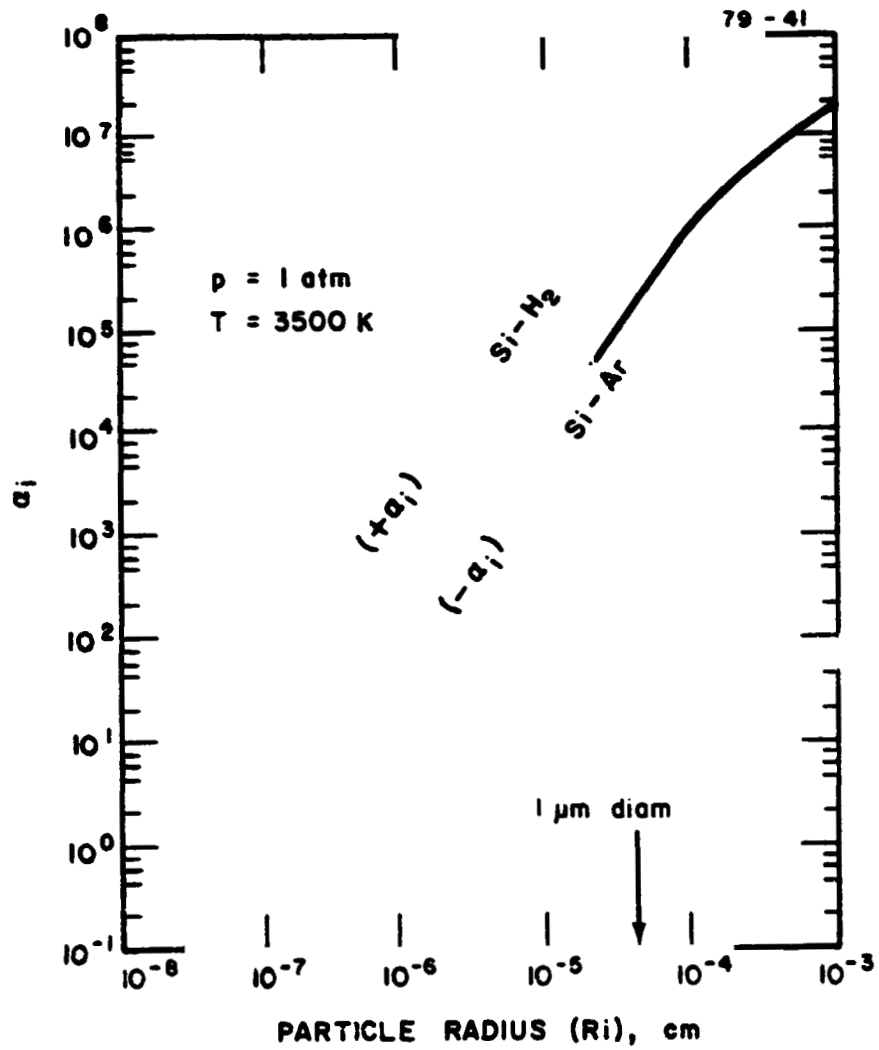


FIGURE 6 COMPARISON OF THE SORLET FACTOR α_i FOR TWO DIFFERENT TYPES OF CARRIER GASES